Within and across fiber temporal fine structure coding following noise induced hearing loss

Sushrut Kale[1], Jon Boley[1], Jayaganesh Swaminathan[2] and Michael G. Heinz[1,2]

[1] Weldon School of Biomedical Engineering and [2] Department of Speech, Language, and Hearing Sciences
Purdue University, West Lafayette, IN 47907

752

1. Introduction:

Recent psychophysical studies have suggested that listeners with sensorineural hearing loss (SNHL) have a reduced ability to use temporal fine-structure cues and that this deficit is correlated with their reduced ability to perceive speech in temporally varying background noise (Hopkins and Moore 2007; Lorenzi et. al. 2006). These perceptual results have renewed an interest in the effects of SNHL on the neural coding of temporal fine structure, both within single auditory-nerve (AN) fibers and across fibers with different characteristic frequencies (CFs). It has been hypothesized that degradation in within fiber phase locking or broadened tuning following SNHL might underlie the perceptual TFS deficits observed in hearing impaired listeners. There is conflicting evidence as to whether within-fiber encoding of fine-structure (i.e., phase locking) is degraded following SNHL (Harrison and Evans 1979; Woolf et. al. 1981). Another hypothesis suggests that degraded across-fiber temporal coding associated with broader tuning and the associated shallower phase response could underlie these perceptual deficits, e.g., as implicated in spatiotemporal theories of speech coding (e.g., Shamma 1985). The present study compared the effects of noise-induced hearing loss on within- and across-fiber TFS coding. Responses of individual AN fibers to frequency-shifted stimuli were used to predict the responses of a population of AN fibers with differing CFs. Shuffled auto- and cross-correlograms were used to quantify across-CF temporal coding in terms of both a neural cross-correlation coefficient and a characteristic delay that estimates the traveling-wave delay between two CFs.

2. Methods:

Å Auditory nerve (AN) recordings were collected from anesthetized chinchillas.

Å A noise induced sensorineural hearing loss was produced by playing a 50 Hz wide noise centered at 2 KHz (Liberman and Dodds, 1984).

Å This resulted in threshold elevation (Fig. 1A) and broadened tuning (Fig 1B).

Å Stimulus set: Speech sentence (ó A boy fell from the w i n d o w . ô), Broadband noise (BBN) and Pure tones at f i b e r s characteristic frequency.

Å Each stimulus was presented with positive and negative polarity in an interleaved manner, which allowed us to quantify temporal fine structure and envelope separately (Joris, 2003).

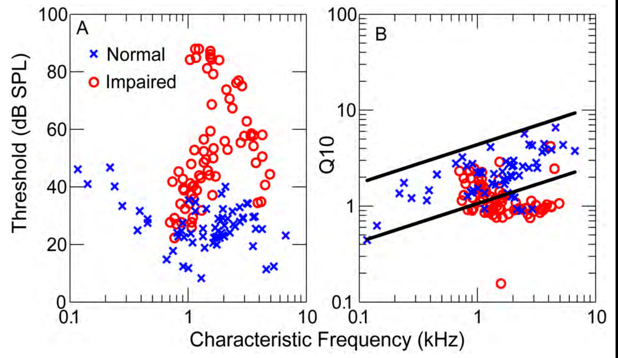

Figure 1: Threshold (A) and Q_{10} (B) vs characteristic frequencies of AN fibers

Spectro-Temporal Manipulation Procedure (STMP)

Å STMP (Heinz, 2007) was used to predict the spatiotemporal population response pattern from responses of single AN fibers.

Å This technique relies on scaling invariance property of the cochlea (Larson et. al., 2008)

Goal: To measure response of fibers with characteristic frequencies ($CF_A=CF_0/1.2$) and ($CF_B=CF_0*1.2$) to $STIM_0$ with sampling frequency F_0

To predict CF_A : $STIM_0$ is played at $1.2*F_0$

To predict CF_B : $STIM_0$ is played at $F_0/1.2$

The response of a below $STIM_0$ neuron (i.e. CF_A) to the baseline $STIM_0$ is predicted by scaling up the measured spike times in response to the shifted $STIM_0$ by a factor of 1.2, thus reducing the effective $STIM_0$ feature frequencies to the baseline values.

Figure 2: Schematic describing STMP procedure

Analysis metrics

Å Shuffled correlograms were used to quantify *within* and *across CF* temporal coding.

Å DIFCORs compare positive and negative stimulus polarities to isolate fine structure

Å Peak height of *shuffled auto-correlogram* DIFCOR quantifies within-fiber TFS coding (Louage et al 2004)

Å The characteristic delay (*CD*) of *shuffled cross-correlogram* estimates traveling-wave delay between two CFs (Joris et al 2006).

Å The effect of CF separation on across-CF correlation and delay was quantified from the predicted spatiotemporal patterns for each AN fiber (figure 4A).

Å For each AN fiber, neural cross-correlation coefficients (ρ_{TFS}) and characteristic delays (CD) were computed for all effective-CF pairs predicted from STMP (figures 4B and C).

Å Width of the region over which TFS was correlated across fibers was quantified as the CF separation at which ρ_{TFS} drops below 0.6 (figure 4C).

Å Traveling wave delay between two fibers separated by 0.5 octaves was compared between normal and impaired population of fibers (figure 4B).

Å Estimates of auditory filters were computed using revcor functions. Revcor functions approximate the impulse response of auditory filter (deBoer and deJongh, 1978; Carney and Yin, 1988).

Å Phase locking to pure tones was quantified using synchronization index (Goldberg and Brown, 1969) and FFT analysis was performed to measure phase responses.

Figure 3: Shuffled correlogram analyses and neural metrics allowed us to selectively quantify temporal fine structure and envelope coding

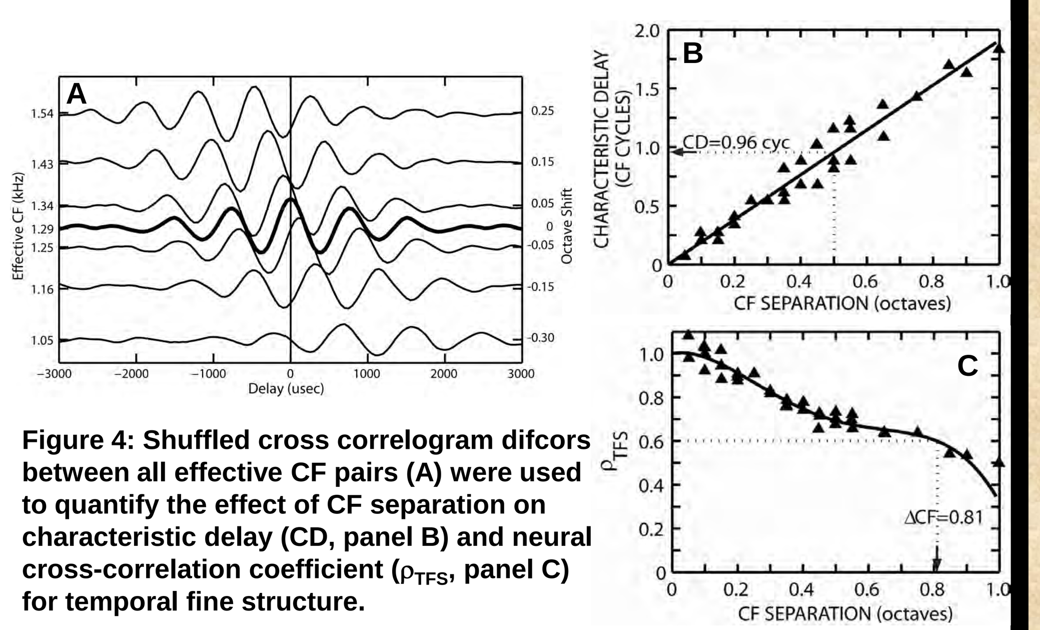

Figure 4: Shuffled cross correlogram difcors between all effective CF pairs (A) were used to quantify the effect of CF separation on characteristic delay (CD, panel B) and neural cross-correlation coefficient (ρ_{TFS}, panel C) for temporal fine structure.

3. Strength of within-fiber phase locking to temporal fine structure was not degraded following SNHL

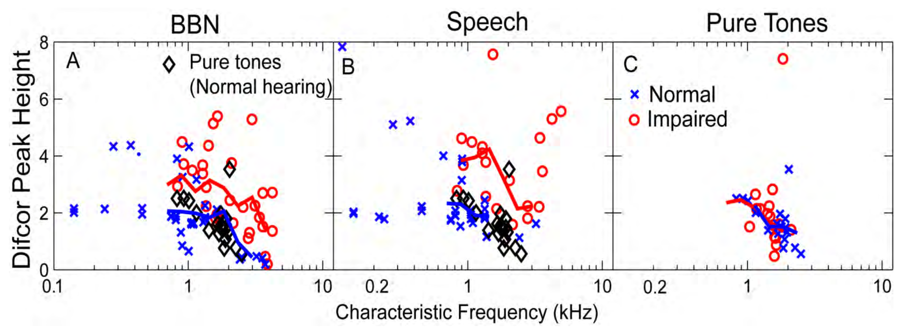

Figure 5: DIFCOR peak heights vs characteristic frequency plotted for broadband noise (A), speech (B) and pure tones (C). Black diamonds indicate DIFCOR peak heights from responses of normal hearing fibers to pure tones (control).

Å Strength of within fiber phase locking as measured by DIFCOR peak heights was not degraded following SNHL for broadband noise, speech and pure tones.

Å Strength of within fiber phase locking to pure tones was comparable between normal hearing and hearing impaired population (Fig 5C).

Å For complex stimuli such as speech, strength of phase locking in hearing impaired fibers was better than normal hearing fibers. These findings are discussed later.

Å Roll off in phase locking at higher characteristic frequencies was comparable between normal hearing and hearing impaired population

4. Cross fiber temporal fine structure (TFS) coding was degraded following noise induced hearing loss

Figure 6: Across-CF coding is compared for a normal and an impaired AN fiber with similar CFs. Following noise induced hearing loss, TFS was correlated over a broader CF region (compare panels B: normal hearing and C: Hearing Impaired).

Å Neural cross correlation for temporal fine structure (ρ_{TFS}) decreased with increasing CF separation (ϕCF) for both normal and impaired fibers

Å Impaired fiber had a wider CF-separation range of correlated activity (ϕCF=0.92 oct.) than a normal fiber (ϕCF=0.31 oct.).

Å Figure 7 summarizes the cross fiber TFS coding for population of normal and impaired fibers. Trend lines are fitted over 0.7 octave wide triangular window.

Å For most normal-hearing fibers, the width of correlated activity was less than 0.45 octaves for both broadband noise and speech.

Å The degradation in across-CF correlation was more significant for speech responses

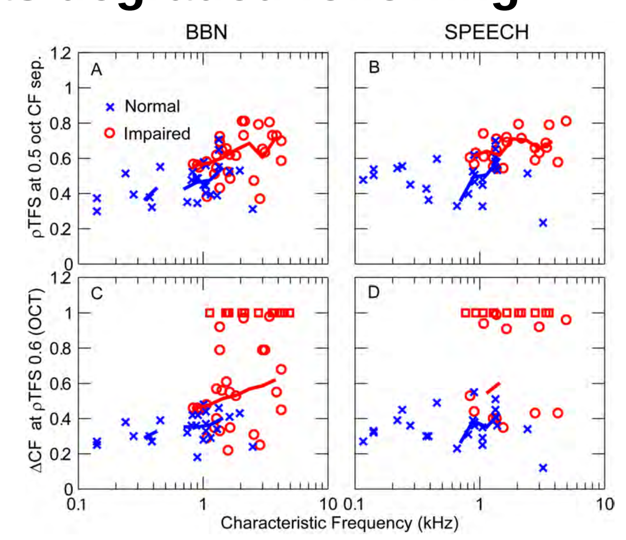

Figure 7: Neural cross correlation (ρ_{TFS}, top row) at ϕCF=0.5 octaves and the smallest CF separation (ϕCF) at which ρ_{TFS} dropped to 0.6 (bottom row) are plotted vs CF for population of normal (blue) and impaired (red) fibers. Squares in panels C and D indicate that ρ_{TFS} never dropped below 0.6 for these fibers even over 1 octave wide ϕCF.

5. Traveling wave delay decreased with SNHL

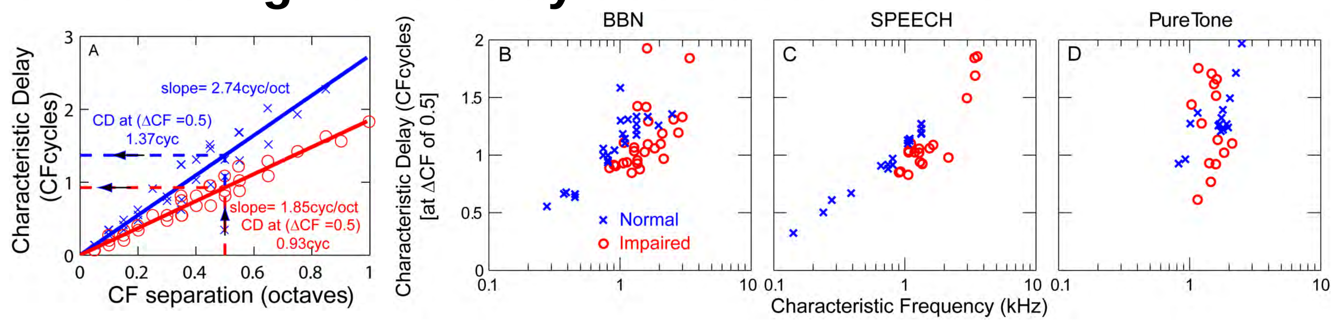

Figure 8: Rate of growth of characteristic delay with ΔCF was slower following SNHL. A) Characteristic delay is plotted as a function of CF separation for a normal (blue) and an impaired fiber (red). Each value in panels B,C and D is the characteristic delay at 0.5 octave CF separation (as shown by dotted lines in panel A).

Å Characteristic Delay (in CF cycles) increased linearly with increasing ϕCF for both normal and impaired fibers (Fig 8A).

Å Impaired fiber had a slower rate of increase (smaller delays).

Å Impaired delays were reduced by ~0.25 CF-cycles for fibers with (1<CF<3 kHz).

Å These quarter cycle shifts in characteristic delays might contribute towards degradation of spatiotemporal cues along the basilar membrane.

6. BF shifts following SNHL contribute to degraded spatiotemporal coding

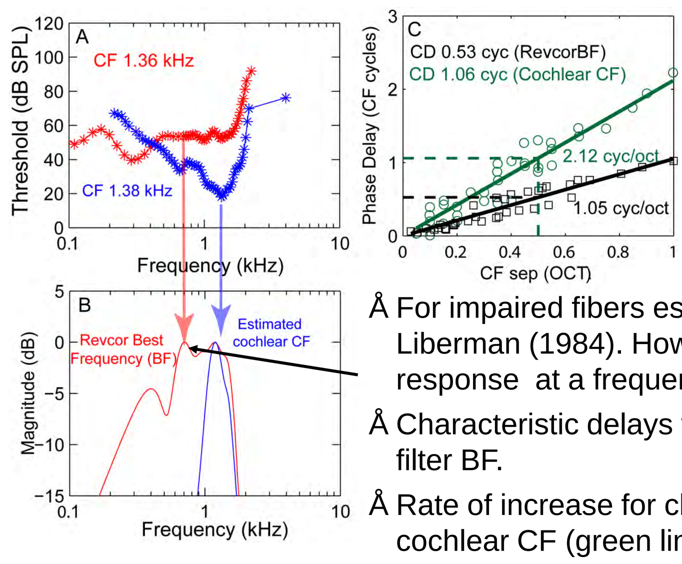

Figure 9: A) Tuning curves and estimates of cochlear characteristic frequency (CF) for a normal (blue) and an impaired fiber. B) Estimates of auditory filters derived from revcor functions computed from neural response of AN fibers for which tuning curve data is shown in A.
C) Characteristic delay computed at estimated cochlear CF (green) and at revcor filter best frequency (black). For a large number of impaired fibers the revcor filter showed maximum response at a frequency more than 0.5 octaves below cochlear CF.

Å For impaired fibers estimated cochlear CF (close match to basilar membrane place CF) was picked according to Liberman (1984). However revcor filter estimates derived for many of the impaired fibers showed maximum response at a frequency much lower than estimated cochlear CF (also see figure 10 A).

Å Characteristic delays were estimated for 9 predicted AN fiber responses around estimated cochlear CF and revcor filter BF.

Å Rate of increase for characteristic delays was shallower around revcor BF (black line, figure 9C) than around cochlear CF (green line).

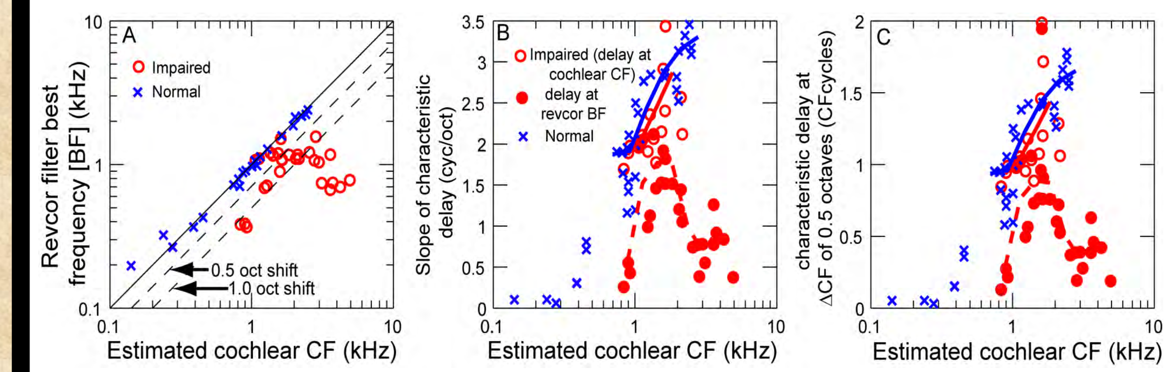

Figure 10: A) Best response frequency of revcor filter estimates is plotted vs estimates of cochlear CF for individual AN fibers. Solid black line indicates a perfect match between revcor filter BF and cochlear CF. Dotted lines indicate deviation from cochlear CF by 0.5 octave and 1 octave. B) Slope of characteristic delay vs octave CF separation function computed at cochlear CF (open red circles for impaired fibers and blue crosses for normal fibers) and at revcor BF (filled red circles). C) Characteristic delay between two fibers with CFs 0.5 octaves apart.

Å For almost all the normal fibers, estimated cochlear CF matched with the best frequency of revcor filters (Fig. 10A)

Å For many impaired fibers revcor filters showed resonant response at much lower frequency, with many revcor filters showing maximum response at a frequency more than an octave below cochlear CF.

Å Phase estimates could not be computed at cochlear CFs of many impaired fibers since revcor filter magnitude response rolled off by more than 20 dB at those frequencies.

Å Phase delay and characteristic delay estimates for such impaired fibers showed consistently slower rate of growth (shallower slope, fig 10C) indicating slower traveling wave delay.

Å This data suggests that the impaired fibers may be more responsive to the energy falling within low frequency (tail) region of their tuning curve excitatory area. This off-frequency listening of the impaired fibers might be the significant factor for shallower phase responses (slower traveling wave delay) and high DIFCOR peak heights that were initially observed (Figures 3 and 5).

7. Phase analyses of tone responses suggest that BF shifts with impairment are a significant factor in reduced traveling-wave delays

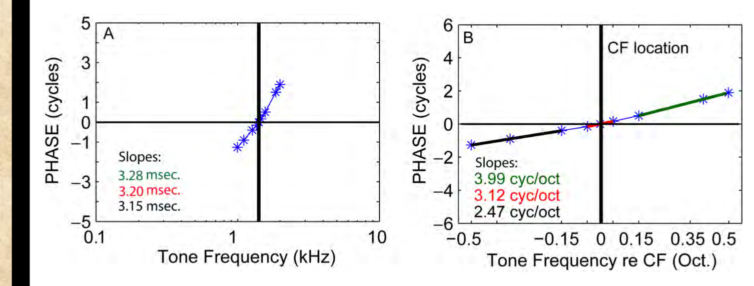

Figure 11: Phase response of 1 normal hearing fiber to 9 pure tones ranging in frequency from 0.5 octave below to 0.5 octave above f i b e r s CF is plotted as a function of tone frequency (A) and separation from CF in octaves (B). Slopes were computed at three different segments of the phase function as shown by black, red and green lines corresponding to below CF, at CF and above CF regions respectively.

Å Slopes of phase vs octave separation f u n c t i o n m e a s u r e d a t f i b e r s CF were steeper than the slopes measured for tones presented 0.5 o c t a v e b e l o w f i b e r s CF.

Å This trend was similar in both, normal and hearing impaired populations and there were no systematic differences in phase slopes between normal and impaired population.

Å Thus, broadened tuning alone, did not seem to contribute to reduced traveling wave delays following SNHL based on the analysis of fixed frequency stimuli like pure tones.

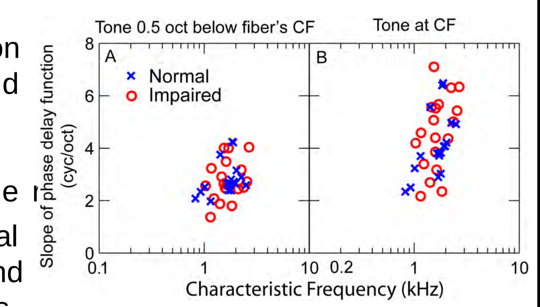

Figure 12: Slope of phase vs octave separation function at CF (panel B) and 0.5 octave below CF (panel A) [see figure 11] is plotted for a population of normal (blue) and impaired (red) fibers.

8. Discussion

Å No degradation was observed in the strength of *within-fiber* temporal fine structure coding

Å Two forms of degradation were observed in *across-fiber* temporal coding:

- Å Broadened CF range over which AN responses were correlated
  - Å l e a d s t o f e w e r ñ i n d e p e n d e n t ò i n f o r m a t i o n c h a n n e l s f o r c o m
- Å Reduced traveling-wave delay
  - Å removes sharp phase-t r a n s i t i o n c u e s i m p l i c a t e d i n m a n y s p a t i o t e m p o r a
  - Å leads to overly coincident temporal features across CFs

Å Shifts in fiber BF following SNHL appear to contribute significantly to these degradations in across-CF coding

- Å Phase responses below cochlear CF (in hypersensitive tail region) are shallower than near CF

Å The effects of SNHL on *across-CF coding* are significant and need to be considered when interpreting the reduced perceptual ability of listeners with SNHL to use fine-structure cues (e.g., Lorenzi et al. 2006; Hopkins and Moore 2007).

9. Acknowledgements

Work supported by research grants from National Organization of Hearing Research Foundation (NOHR) and NIH (R01-DC09838).

10. References:

Carney LH, Yin TC. Temporal coding of resonances by low-frequency auditory nerve fibers: single-fiber responses and a population model. J Neurophysiol 60:1653-1677, 1988.
de Boer E, de Jongh HR. On cochlear encoding: potentialities and limitations of the reverse-correlation technique. J Acoust Soc Am 63:115-135, 1978.
Goldberg JM, Brown PB. Response of binaural neurons of dog superior olivary complex to dichotic tonal stimuli: some physiological mechanisms of sound localization. J Neurophysiol 32:613-636, 1969.
Harrison RV, Evans EF. Some aspects of temporal coding by single cochlear fibres from regions of cochlear hair cell degeneration in the guinea pig. Arch Otorhinolaryngol 224:71-78, 1979.
Heinz MG. Spatiotemporal encoding of vowels in noise studied with the responses of individual auditory nerve fibers. In: Kollmeier B, Klump G, Hohmann V, Langemann U, M. Mauermann, Uppenkamp S, Verhey J (eds) Hearing ï From Sensory Processing to Perception. Springer-Verlag, Berlin, pp 107-115, 2007.
Heinz MG, Swaminathan J. Quantifying envelope and fine-structure coding in auditory-nerve responses to chimaeric speech. J Assoc Res Otolaryngol 10:407-423, 2009.
Hopkins K, Moore BC. Moderate cochlear hearing loss leads to a reduced ability to use temporal fine structure information. J Acoust Soc Am 122:1055-1068, 2007.
Joris PX. Interaural time sensitivity dominated by cochlea-induced envelope patterns. J Neurosci 23:6345-6350, 2003.
Joris PX, Van de Sande B, Louage DH, van der Heijden M. Binaural and cochlear disparities. Proc Natl Acad Sci USA 103:12917-12922, 2006.
Larsen E, Cedolin L, Delgutte B. Pitch representations in the auditory nerve: two concurrent complex tones. J Neurophysiol 100:1301-1319, 2008.
Liberman MC. Single-neuron labeling and chronic cochlear pathology. I. Threshold shift and characteristic-frequency shift. Hear Res 16:33-41, 1984.
Liberman MC, Dodds LW. Single-neuron labeling and chronic cochlear pathology. III. Stereocilia damage and alterations of threshold tuning curves. Hear Res 16:55-74, 1984.
Lorenzi C, Gilbert G, Carn H, Garnier S, Moore BC. Speech perception problems of the hearing impaired reflect inability to use temporal fine structure. Proc Natl Acad Sci USA 103:18866-18869, 2006.
Louage DH, Van Der Heijden M, Joris PX. Temporal properties of responses to broadband noise in the auditory nerve. J Neurophysiol 91:2051-2065, 2004.
Shamma SA. Speech processing in the auditory system. I: The representation of speech sounds in the responses of the auditory nerve. J Acoust Soc Am 78:1612-1621, 1985.
Woolf NK, Ryan AF, Bone RC. Neural phase-locking properties in the absence of cochlear outer hair cells. Hear Res 4:335-346, 1981.